Zhang *et al. Chem Synth* 2024;4:xx
DOI: 10.20517/cs.2023.37

Chemical Synthesis

Supplementary Materials

Constructing a hierarchical MoS_2/MXene heterostructure for efficient capacitive deionization of saline water

Youfang Zhang[1], Xin Li[1], Wen Xi[2], Qi Zhang[1], Xiaohui Ge[1], Jun You[1], Qunchao Zhang[1], Dean Shi[1,*], Jun Jin[2,*]

[1]Hubei Key Laboratory of Polymer Materials, Ministry of Education Key Laboratory for Green Preparation and Application of Functional Materials, School of Materials Science and Engineering, Hubei University, Wuhan 430062, Hubei, China.
[2]Faculty of Materials Science and Chemistry, China University of Geosciences, Wuhan 430074, Hubei, China.

[*]**Correspondence to:** Prof. Dean Shi, Hubei Key Laboratory of Polymer Materials, Ministry of Education Key Laboratory for Green Preparation and Application of Functional Materials, School of Materials Science and Engineering, Hubei University, 368 Youyi Avenue, Wuchang District, Wuhan 430062, Hubei, China. E-mail: deanshi2012@hubu.edu.cn; Prof. Jun Jin, Faculty of Materials Science and Chemistry, China University of Geosciences, 388 Lumo Road, Hongshan District, Wuhan 430074, Hubei, China. E-mail: jinjun@cug.edu.cn

EXPERIMENTAL

Materials

Ti_3AlC_2 powders (98 wt% purity) are purchased from 11 Technology (Co., Ltd.). Thiourea (AR, 99%) and ammonium molybdate tetrahydrate ($(NH_4)_6Mo_7O_{24}·4H_2O$, AR, 99%) are purchased from Shanghai Macklin Biochemical (Co., Ltd.). HF (AR, ≥ 40%), 1-methyl-2-pyrrolidone (NMP, AR), active carbon (AC), NaCl, and polyvinylidene fluoride (PVDF) are obtained from Sinopharm Chemical Reagent Co., Ltd. All the regents are used without any pretreatment.

Preparation of MXene nanosheets

Briefly, 2 g of Ti_3AlC_2 is slowly added to a 10% HF aqueous solution with magnetic stirring for 24 h. Afterwards, the black precipitate is collected and washed with deionized water and ethanol, respectively, until the pH of the solution reaches neutral through centrifugation. The MXene nanosheets are obtained by vacuum drying at 60 °C for 24 h and stored in an N_2 atmosphere for subsequent use.

Characterization

The structures and morphologies of the as-prepared hierarchical MoS_2/MXene heterostructure samples are investigated using a field emission scanning electron microscope (FESEM, ZEISS-Sigma 500-0627). The chemical composition is characterized by the energy dispersive X-ray spectroscopy (EDX). X-ray diffraction (XRD) patterns are performed on an X' Pert Pro X-ray diffractometer with Cu Kα radiation (λ = 0.1542 nm) under a current of 40 mA and a voltage of 40 kV with 2θ ranges from 5° to 80°. X-ray photoelectron spectroscopy (XPS) spectra are collected by a spectrometer (Thermo scientific ESCAlab 250xi) using monochromatic Al Ka X-ray radiation. The quantification and peak fitting of the core-level spectra are performed using a software package (Thermo Avantage v5.986). The wettability and contact angle measurements are conducted using a contact angle analyzer (OCA25, Germany) with DI water as the probe liquids.

Electrochemical measurements

The details of electrochemical characterizations are described in the Supplementary Materials.

To investigate the performance of MoS_2/MXene as CDI electrode material, a mixture of MoS_2/MXene heterostructure, PVDF and conductive carbon black in a ratio of 7:2:1 is mixed in N-methyl pyrrolidinone (NMP) with magnetic stirring for 12 h to form a slurry. The slurry is then cast on a 1 × 6 cm^2 graphite paper with an effective area of 1 × 2 cm^2 and dried in a vacuum oven to obtain the hierarchical MoS_2/MXene heterostructure working electrode. The cyclic voltammetry (CV), electrochemical impedance spectroscopy (EIS) and galvanostatic charge/discharge (GCD) are performed in a 1 M NaCl solution using the three-electrode method on an electrochemical work station (Chenhua CHI600E). The three-electrode system is composed of the working electrode, platinum counter electrode, Ag/AgCl reference electrode, and 1.0 M NaCl electrolyte.

The specific capacitance (C, $F \cdot g^{-1}$) is calculated from the CV curves according to the following equation (Eq. 1):

$$C = \int \frac{IdV}{2vm\Delta V} \quad (1)$$

Where I, v, m, and ΔV represent the current (A), scan rate ($mV \cdot s^{-1}$), mass of active material (g), and potential window (V), respectively.

The specific capacitance (C, $F \cdot g^{-1}$) is calculated from the GCD curves according to the following equation (Eq. 2):

$$C = \frac{I*\Delta t}{m*\Delta V} \quad (2)$$

Where I, Δt, m, and ΔV represent the current (A), discharge time (s), mass of active material (g), and potential window (V), respectively.

Desalination measurements

The desalination measurements are carried out using a batch-mode circulation system. The CDI system consists of the hierarchical MoS_2/MXene heterostructure as an anode, a cation exchange membrane (CEM), a spacer, an anion exchange membrane (AEM), and active carbon as a cathode. The CEM selectively permeates cations, while the AEM selectively permeates anions. The effective size of the cathodes for desalination is adjusted to 4 × 4 cm^2. During the desalination process, a peristaltic pump is used to flow the NaCl solution into the CDI module at a rate of 20 $mL \cdot min^{-1}$. The initial conductivities of NaCl solution are set to 500 or 1,000 $\mu S \cdot cm^{-1}$. In addition, a power

supply with a voltage of 0.8-1.2 V is applied to both the anode and cathode of the CDI module. The desalination capacity (Q, mg·g^{-1}), average desalination rate (v, mg·g^{-1}·min^{-1}), and charge efficiency (Λ, %) are calculated according to the following equation (Eq. 3):

$$Q = \frac{(C_0 - C_e) \times V}{m} \quad (3)$$

where Q, C_0, C_e, V, and m represent the electro-sorption capacity (mg·g^{-1}), initial and equilibrium concentration (mg·L^{-1}) of NaCl solution, volume of NaCl solution, and mass (g) of active material, respectively.

The average desalination rate (v, mg g^{-1} min^{-1}) is calculated according to (Eq. 4):

$$v = \frac{Q}{t} \quad (4)$$

where t refers to the adsorption time (min).

The charge efficiency (Λ, %) is calculated according to (Eq. 5, Eq. 6):

$$\Lambda = \frac{\mathrm{Q} \times m \times F}{1000 \times \mathrm{M} \times \Sigma} \quad (5)$$

$$\Sigma = \int I dt \quad (6)$$

where Λ, F, M, Σ, and I represent the charge efficiency, Faraday constant (96,485 C·mol^{-1}), molar mass of NaCl (58.4 g·mol^{-1}), integration (C·g^{-1}) of the current during the ion adsorption step, and current (A), respectively.

Supplementary Table 1. Elemental contents of MoS_2/MXene-2 heterostructure obtained from XPS

Element	Ti	C	Mo	O	S
Content (%)	3.12	22.74	20.21	24.93	28.99

Supplementary Table 2. Comparison of various MoS_2 based electrode materials for CDI applications

Materials	CDI model layout	Voltage (V)	Initial concentration of NaCl ($mg \cdot L^{-1}$)	Capacity ($mg \cdot g^{-1}$)	Maximum desalination rate ($mg \cdot g^{-1} \cdot min^{-1}$)	Ref.
MoS_2/MXene heterostructure	MoS_2/MXene‖AC	1.2	500	55.8	15.2	This work
MoS2/rGO	MoS2/rGO‖AC	1.0	200	16.82	-	[1]
Defected-MoS_2/rGO	MoS_2/rGO‖AC	0.8	200	25.47	-	[2]
Exfoliated MoS_2	MoS_2‖AC	1.2	400	8.81	-	[3]
MoS_2@CNT-CS	CNT-CS‖MoS_2@CNT-CS	1.2	500	25.35	3.9	[4]
MoS_2/MXene	MoS_2/MXene‖AC	1.2	500	23.98	4.6	[5]
CNFs@ MoS_2	CNFs@ MoS_2‖AC	1.2	3,000	53.03	9.42	[6]
MoS_2@NCS	MoS_2@NCS‖AC	1.4	2,000	59.9	-	[7]
MoS_2/NOMC	MoS_2/NOMC‖AC	1.6	250	28.82	-	[8]
rGO@PEI/MoS_2	rGO@PEI/MoS_2‖AC	1.0	200	24.13	-	[9]

CNT: Carbon nanotubes; CS: carbon spheres; CNFs: carbon nanofibers; NCS: N-doped carbon sphere; NOMC: nitrogen-doped highly ordered mesoporous carbon; PEI: positively charged polyethyleneimine.

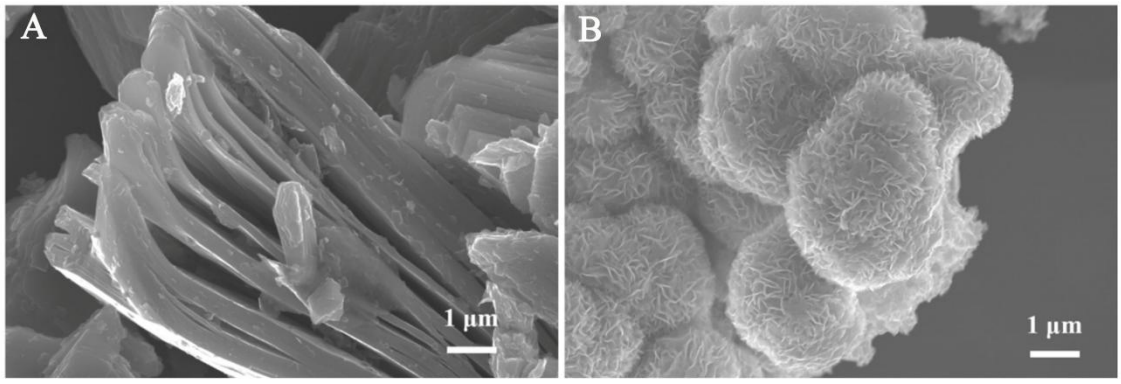

Supplementary Figure 1. SEM images of MXene (A) and pure MoS_2 (B).

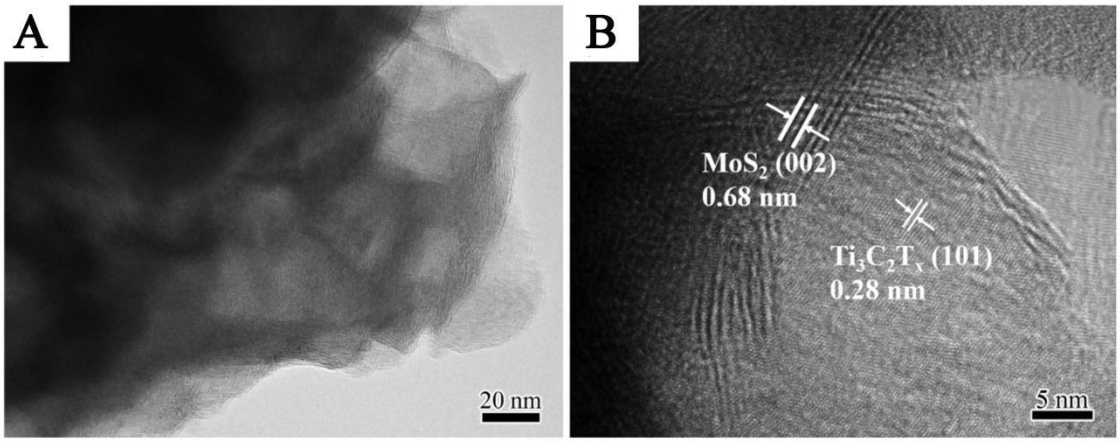

Supplementary Figure 2. TEM (A) and HRTEM images (B) of MoS_2/MXene-2 heterostructure.

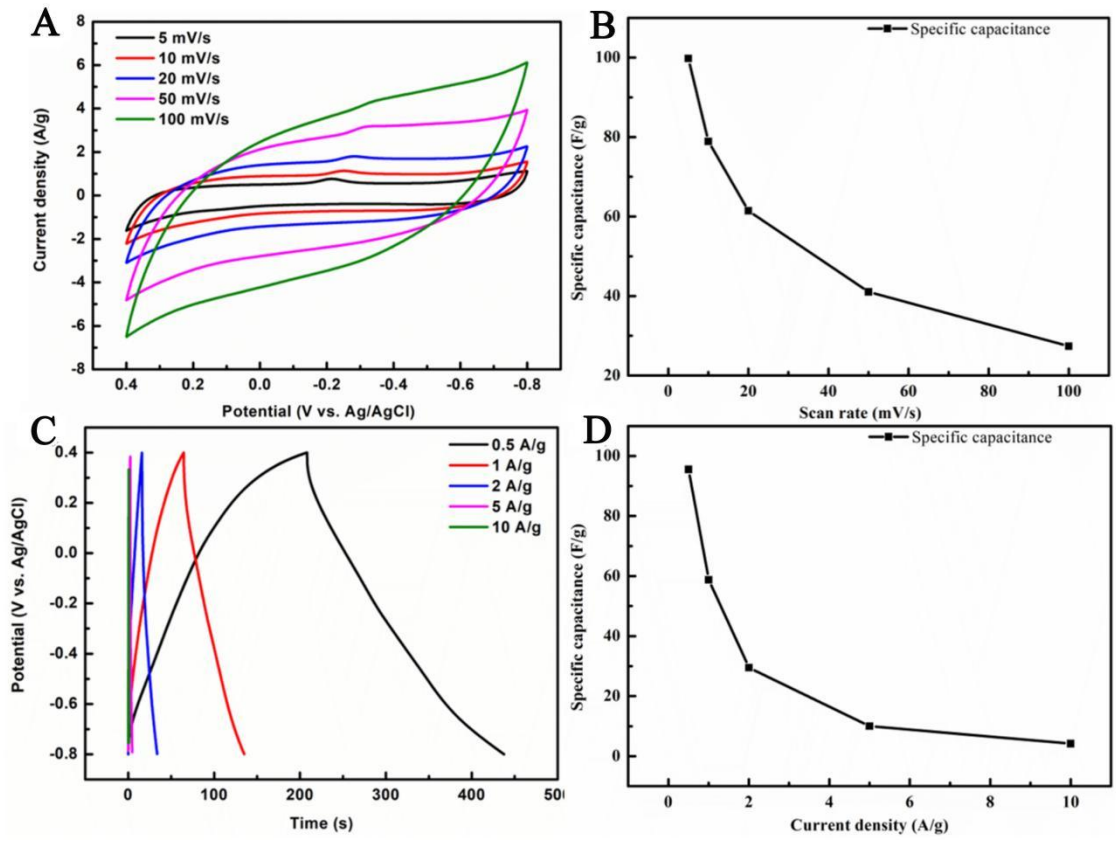

Supplementary Figure 3. CV curves of MoS_2 at various scan rates (A), the specific capacitances calculated from CV curves (B), GCD curves of MoS_2 at various current densities (C), and the specific capacitances calculated from GCD curves (D).

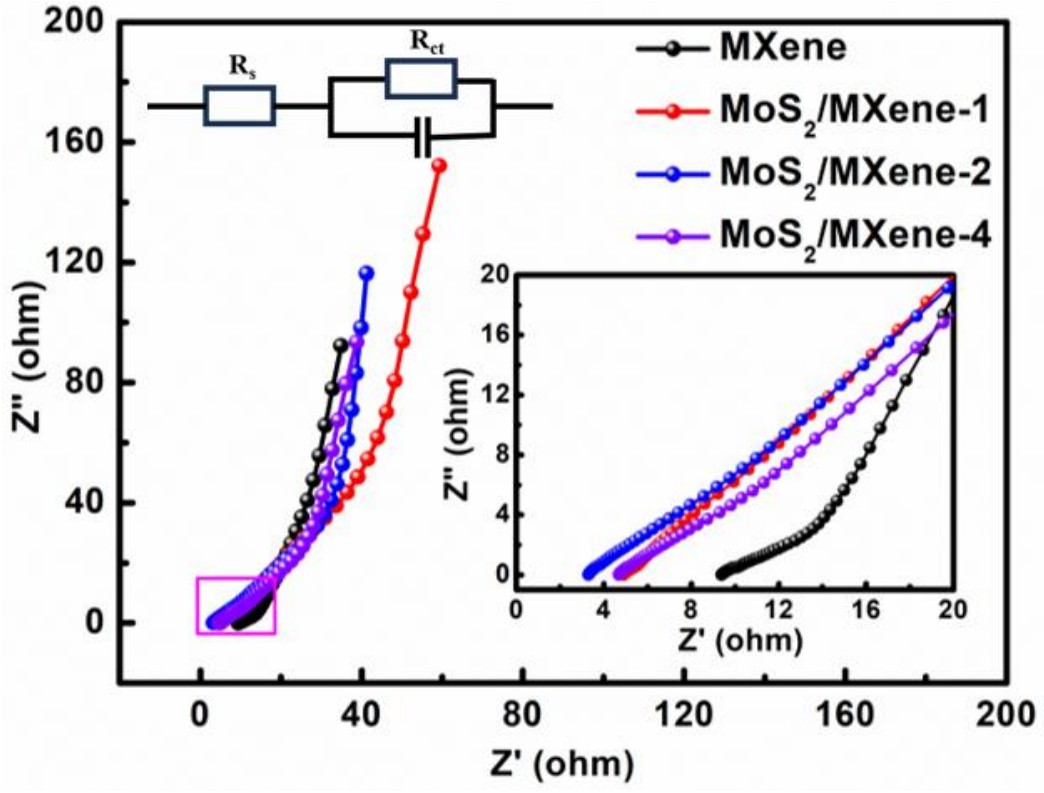

Supplementary Figure 4. EIS Nyquist plots of MXene and hierarchical MoS_2/MXene heterostructures.

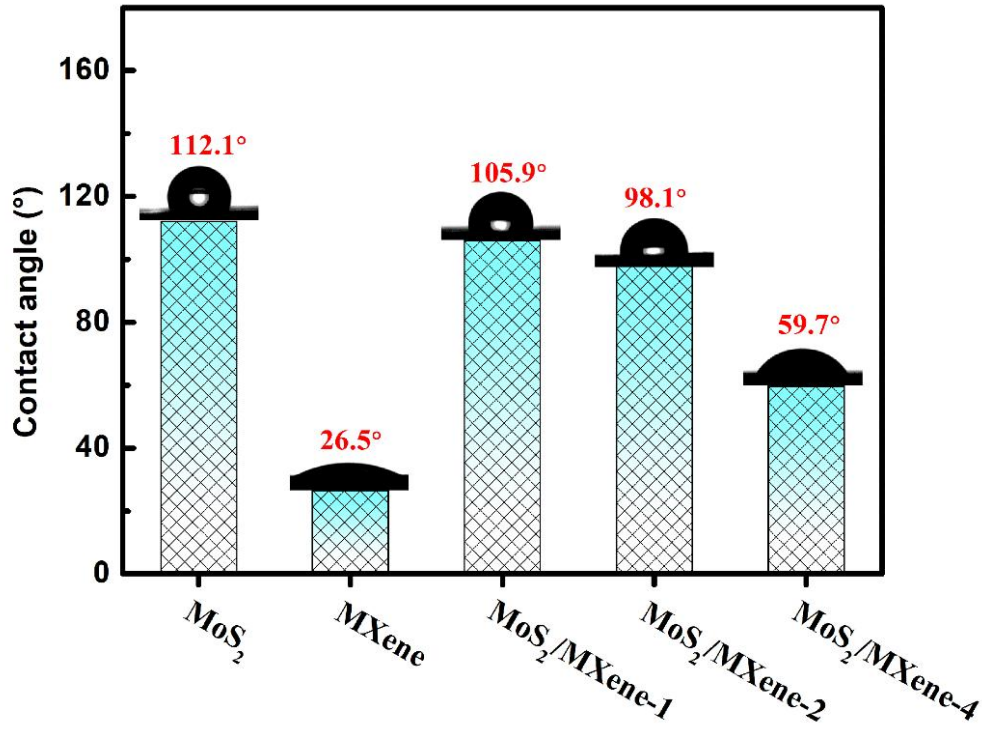

Supplementary Figure 5. Water contact angles of pure MoS_2, MXene and hierarchical MoS_2/MXene heterostructures.

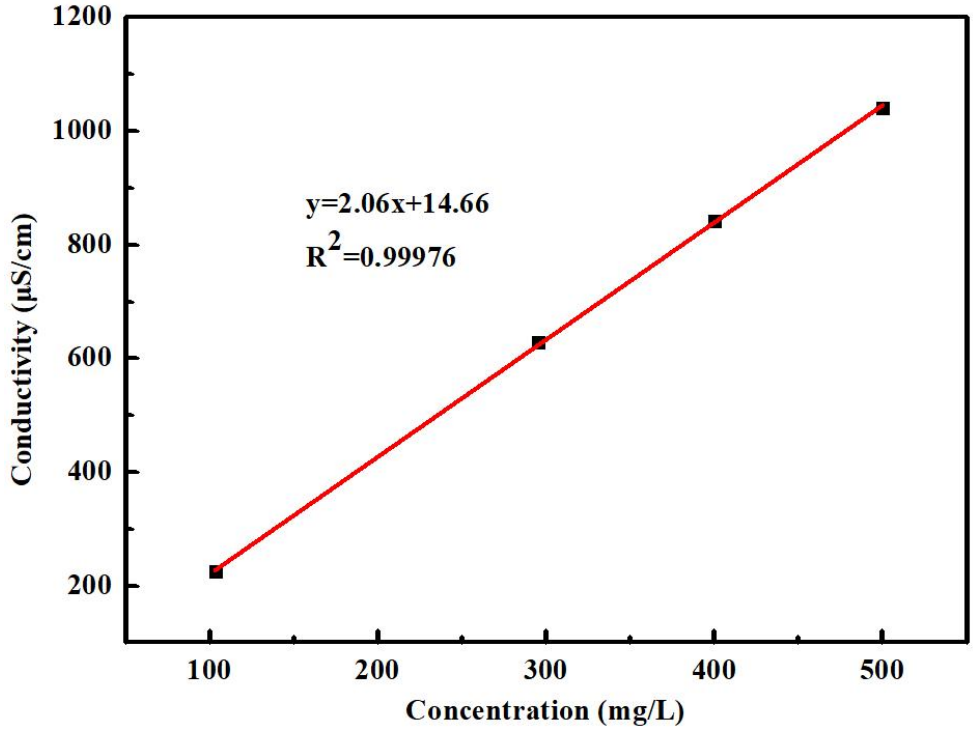

Supplementary Figure 6. The relationship between the conductivity of NaCl solution and its concentration at room temperature.

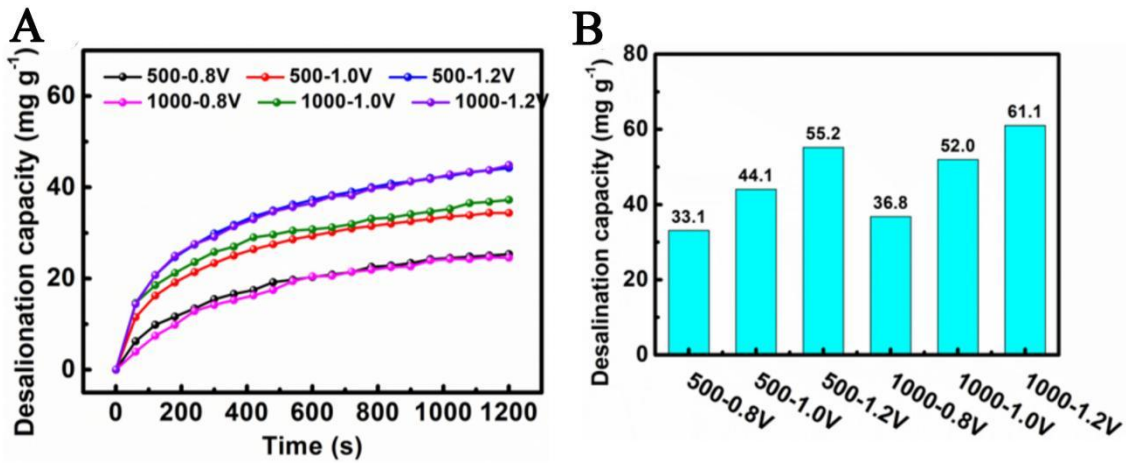

Supplementary Figure 7. The desalination capacity and time curves of MoS_2 (A) and the desalination capacities of MoS_2 (B).

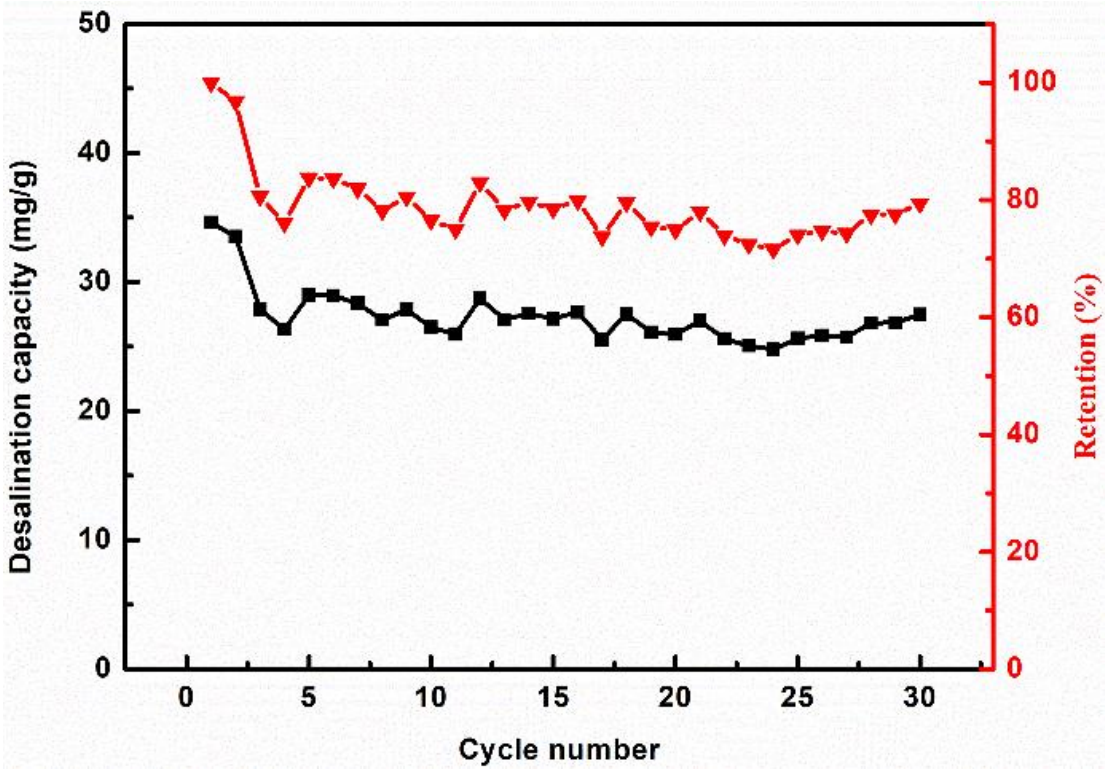

Supplementary Figure 8. The cycling performance of the MoS_2/MXene-2 heterostructure electrode in NaCl solution with an initial conductivity conductivity of 500 $\mu S \cdot cm^{-1}$ at 1.2 V.

References

1. Peng WJ, Wang W, Han Gh, Huang Yk, Zhang YS. Fabrication of 3D flower-like MoS_2/graphene composite as high-performance electrode for capacitive deionization. *Desalination* 2020; 473: 114191. https://doi.org/10.1016/j.desal.2019.114191

2. Peng WJ, Wang W, Qi MY, Miao YH, Huang YK, Yu FT. Enhanced capacitive deionization of defect-containing MoS_2/graphene composites through introducing appropriate MoS_2 defect. *Electrochim. Acta* 2021; 383: 138363. https://doi.org/10.1016/j.electacta.2021.138363

3. Xing F, Li T, Li JY, Zhu HR, Wang N, Cao X. Chemically exfoliated MoS_2 for capacitive deionization of saline water. *Nano Energy* 2017; 31: 590-595. https://doi.org/10.1016/j.nanoen.2016.12.012

4. Cai YM, Zhang W, Fang RL, Zhao DD, Wang Y, Wang JX. Well-dispersed few-layered MoS_2 connected with robust 3D conductive architecture for rapid capacitive deionization process and its specific ion selectivity. *Desalination* 2021; 520: 115325. https://doi.org/10.1016/j.desal.2021.115325

5. Chen ZQ, Xu XT, Liu Y, et al. Ultra-durable and highly-efficient hybrid capacitive deionization by MXene confined MoS_2 heterostructure. *Desalination* 2022; 528: 115616. https://doi.org/10.1016/j.desal.2022.115616

6. Liu Y, Du X, Wang ZP, et al. MoS_2 nanoflakes-coated electrospun carbon nanofibers for “rocking-chair” capacitive deionization. *Desalination* 2021; 520: 115376. https://doi.org/10.1016/j.desal.2021.115376

7. Nguyen, T. K. A.; Wang, T.-H.; Doong, R.-A., Architectures of flower-like MoS_2 nanosheet coated N-doped carbon sphere electrode materials for enhanced capacitive deionization. *Desalination* 2022, *540*. https://doi.org/10.1016/j.desal.2022.115979

8. Tian SC, Zhang XH, Zhang ZH. Novel MoS_2/NOMC electrodes with enhanced capacitive deionization performances. *Chem. Eng. J.* 2021; 409: 128200. https://doi.org/10.1016/j.cej.2020.128200

9. Zheng PK, Wang L, Wang QM, Zhang JF. Enhanced capacitive deionization by rGO@PEI/MoS_2 nanocomposites with rich heterostructures. *Sep. Purif. Technol.* 2022; 295: 121156. https://doi.org/10.1016/j.seppur.2022.121156